

# Synthesis, molecular modeling, and biological evaluation of 1,2,4-triazole derivatives containing pyridine as potential anti-tumor agents

Yan-Bin Zhang · Wen Liu · Yu-Shun Yang ·  
Xiao-Liang Wang · Hai-Liang Zhu ·  
Li-Fei Bai · Xiao-Yang Qiu

Received: 27 July 2012 / Accepted: 24 October 2012 / Published online: 15 November 2012  
© Springer Science+Business Media New York 2012

**Abstract** There is an accumulating body of experimental evidences validating focal adhesion kinase (FAK) as a therapeutic target and offering opportunities for anti-tumor drug development. In present study, we sought to synthesize twenty-eight potential FAK inhibitors as anti-tumor agents based on 1,2,4-triazole skeleton. The bioassay assays demonstrated that compounds **3e** and **6j** showed the most potent activity, **3e** inhibited the growth of HCT116 and HepG2 cell lines with  $IC_{50}$  values of 8.17 and 7.04  $\mu$ M, while compound **6j** showed the most potent biological activity against HCT116 cell line ( $IC_{50} = 1.99 \mu$ M). Besides, compound **6j** also exhibited significant FAK inhibitory activity ( $IC_{50} = 2.41 \mu$ M). The results of flow cytometry and western-blot assay demonstrated that compounds **3e** and **6j** possessed good anti-proliferative activity. Docking simulations were performed to position compounds **3e** and **6j** into the active site of FAK to determine the probable binding model.

**Keywords** FAK · 1,2,4-triazole · Anti-tumor activity · Molecular docking

## Introduction

Cancer, the second leading cause of death in the world, is continuing to be a major health problem in developing as well as undeveloped countries (EI-Azab *et al.*, 2010). Cancer chemotherapy targeting tumor progression represents one of the most relevant challenges of chemists and oncologist. In order to gain new insights into the complexity of the disease, robust screening methods for evaluating different natural or synthetic drugs have been carried out from the science community (Stanton *et al.*, 2008). Therefore, there is an increasing need for new therapies, especially those that based on current knowledge of cancer biology as well as that taking advantage of the cancer cells phenotype, described by Hanahan and Weinberg (2000).

The non-receptor protein tyrosine kinase focal adhesion kinase (FAK) was discovered almost 15 years ago (Van Nimwegen and van de Water, 2007). Most studies show an enhanced expression of FAK mRNA and/or protein in a variety of human cancers, including squamous cell carcinoma of the larynx (Aronsohn *et al.*, 2003), invasive colon and breast tumors (Owens *et al.*, 1995), and malignant melanoma (Kahana *et al.*, 2002). Activation of FAK leads to a number of cell biological processes, including cell attachment, migration, invasion, proliferation, and survival (Maroesja and Bob, 2007). The human FAK core promoter contains binding sites for many transcription factors, including but not limited to NF- $\kappa$ B, p53, AP-1, AP-2, PU.1, TCF-1, and EGR-1 (Golubovskaya *et al.*, 2004). Inhibition of FAK by anti-sense techniques or antibody-methods results in the onset of apoptosis and numerous studies have clearly confirmed a protective role for FAK in apoptosis (Sonoda *et al.*, 2000). Given the role of FAK in processes important in

Y.-B. Zhang · W. Liu · Y.-S. Yang · X.-L. Wang ·  
H.-L. Zhu (✉)

State Key Laboratory of Pharmaceutical Biotechnology, Nanjing University, 210093 Nanjing, People's Republic of China  
e-mail: zhuhl@nju.edu.cn

L.-F. Bai (✉)

School of Life Sciences and Chemistry, Jiangsu Institute of Education, 210013 Nanjing, People's Republic of China

X.-Y. Qiu (✉)

Department of Chemistry, Shangqiu Normal University, 476000 Shangqiu, People's Republic of China

tumorigenesis, metastasis, and the link to prominent oncogenes, FAK might be a promising target in the ongoing search for an anti-cancer drug (Maroesja and Bob, 2007).

The chemistry of N-bridged heterocycles derived from 1,2,4-triazole has received considerable attention in recent years due to their usefulness in different areas of biological activities and as industrial intermediates (Bhat *et al.*, 2009). 1,2,4-triazole derivatives are known to exhibit anti-microbial (Ashok and Holla, 2007; Prasad *et al.*, 2009), anti-tubercular (Walczak *et al.*, 2004), anti-cancer (Sztanke and Tuzimski, 2008; Romagnoli and Baraldi, 2010), anti-convulsant (Amir and Shikha, 2004), anti-inflammatory, and analgesic properties (Almasirad *et al.*, 2004). 1,2,4-triazole nucleus has been incorporated into a wide variety of therapeutically interesting drug candidates including H1/H2 histamine receptor blockers, cholinesterase active agents, CNS stimulants, anti-anxiety, and sedatives (Schreier and Helv, 1976), anti-mycotic activity such as fluconazole, itraconazole, and voriconazole (Budavari *et al.*, 1996; Haber, 2001). Some 1,3,4-thiadiazole derivatives have been reported as potential FAK inhibitors (Juan *et al.*, 2011). Pyridine was used to replace benzo[b]dioxin mainly according to the result of CADD (computer assistant drug design) method. The result indicated that a smaller moiety with higher electronic density might improve the bioactivity. Herein, in continuation to extend our research on anti-tumor compounds with FAK structure inhibitory activity, in the present study we sought to synthesis two series of 1,2,4-triazole derivatives containing pyridine as anti-tumor agents. Biological evaluation indicated that some of the synthesized compounds were potent inhibitors of FAK structure.

## Results and discussion

### Chemistry

In this study, twenty-eight triazole derivatives containing pyridine were synthesized. The synthetic route of compounds **3a–3n** and **6a–6n** was shown in Scheme 1. It was prepared in six steps. First, a mixture of corresponding isoniazid and phenyl isothiocyanate was refluxed in ethanol for 30 min. The solution was cooled and compound **1** was precipitated. A solution of NaOH (2 N) containing **1** was stirred under refluxing for 30 min, yielding the desired compound **2** according to the reported procedure. Then, fourteen 1,2,4-triazole derivatives (**3a–3n**) were prepared by refluxing in anhydrous acetonitrile of **2** with different benzyl bromide compounds as shown in Scheme 1 according to the literature. To a solution of compound **2** in acetone, ethyl bromoacetate was added and the mixture

was refluxed for 2 h in the presence of  $K_2CO_3$ . The solution was cooled and compound **4** appeared. Then, compound **5** was prepared by treatment of **4** with hydrazine hydrate (85 %) in ethanol. Finally, fourteen 1,2,4-triazole derivatives (**6a–6n**) were collected by stirring in ethanol of **5** with different benzaldehyde compounds as shown in Scheme 1.

All of the synthetic compounds gave satisfactory analytical and spectroscopic data, which were in full accordance with their depicted structures. Furthermore, the crystal data, data collection, and refinement parameter for compound are listed in Table 1, and Fig. 1 gives a perspective view of this compound together with the atomic labeling system. The structure was solved by direct methods and refined on F2 by full-matrix least-squares methods using SHELX-97 (Sheldrick, 1997).

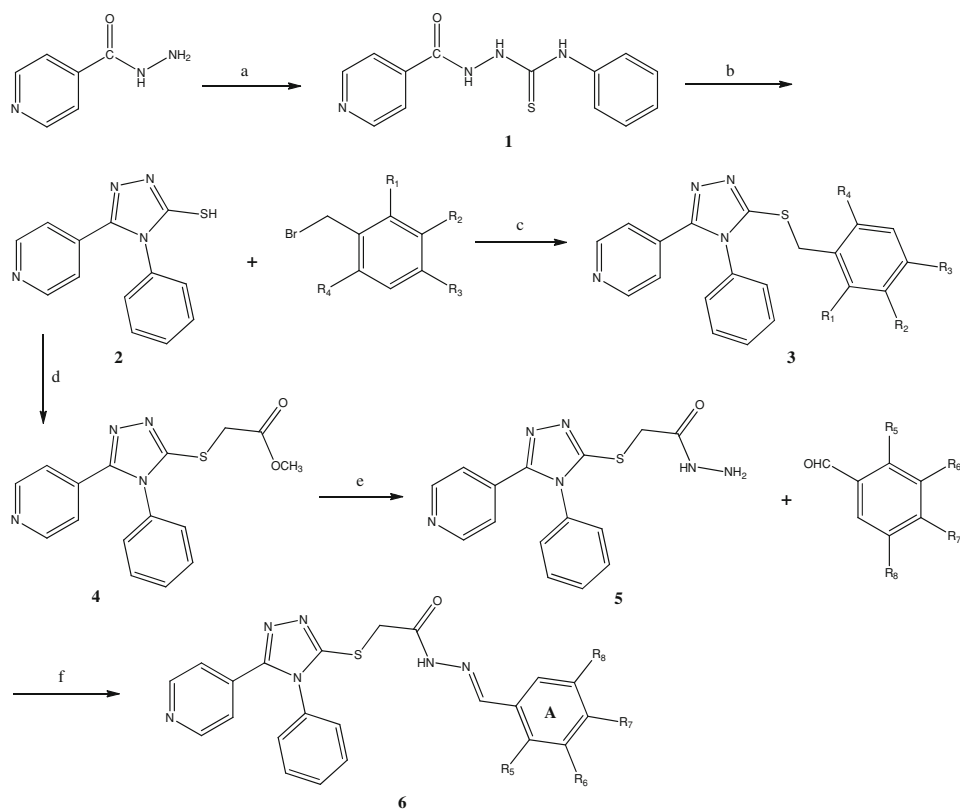
### Biological activity

All the synthesized derivatives **3a–3n** and **6a–6n** were evaluated for their anti-proliferative activity against MCF7 (human breast cancer cells), HCT116 (human colorectal cancer cells), and HepG2 (human hepatoma cells) cell lines. The results were summarized in Table 2. As illustrated in Table 2, compounds **3a–3n** and **6a–6n** showed all certain activities against the three tumor cells as compared with staurosporine. For the studied compounds, we observed that compounds (**3e**, **6j**) showed potent anti-cancer activities against MCF7, HCT116, and HepG2 cell lines. It was obvious that compound **6j** exhibited best activity against HCT116 cells with the  $IC_{50}$  value of 1.99  $\mu M$ , which was even better than the reference drug staurosporine ( $IC_{50} = 13.20 \mu M$ ).

Structure–activity relationships (SARs) in these 1,2,4-triazole derivatives demonstrated that compounds having halogen atom substituent exhibited high activity. Meanwhile, a comparison of the substitution on benzene ring was demonstrated as follows (**3a–3n**): when the compounds were bromine-substituted derivatives, the potency order was *meta* > *para* > *ortho* (**3c**, **3e**, **3h**), and when the compounds were chlorine-substituted derivatives, the potency order was also *meta* > *para* > *ortho* (**3b**, **3d**, **3g**). Interestingly, among the electron-withdrawing substituents compounds, the potency order was almost bromine > chlorine > fluorine > nitro. Another comparison of the substitution on benzene ring was demonstrated as follows (**6a–6n**): compounds with electron-donating substituents at *para*-position at A-ring had better inhibitory activity than that with electron-withdrawing substituents at the same position. When the compounds were fluorine-substituted derivatives, the potency order was *para* > *ortho* > *meta* (**6g**, **6h**, **6i**), among the electron-withdrawing substituents compounds, the potency order was

**Scheme 1** General synthesis of compounds (**3a–3n** and **6a–6n**).

Reagents and conditions:  
**a** Phenyl isothiocyanate, ethanol, reflux, 30 min;  
**b** NaOH (2 N), reflux, 30 min.  
**c** Reflux, acetonitrile.  
**d** Bromoacetate, K<sub>2</sub>CO<sub>3</sub>, acetone, reflux, 2 h. **e** Hydrazine hydrate (85 %), ethanol, rt, 8–12 h; **f** Ethanol, rt

**3a** R<sub>1</sub>=F, R<sub>2</sub>=R<sub>3</sub>=R<sub>4</sub>=H**3b** R<sub>1</sub>=Cl, R<sub>2</sub>=R<sub>3</sub>=R<sub>4</sub>=H**3c** R<sub>1</sub>=Br, R<sub>2</sub>=R<sub>3</sub>=R<sub>4</sub>=H**3d** R<sub>2</sub>=Cl, R<sub>1</sub>=R<sub>3</sub>=R<sub>4</sub>=H**3e** R<sub>2</sub>=Br, R<sub>1</sub>=R<sub>3</sub>=R<sub>4</sub>=H**3f** R<sub>3</sub>=F, R<sub>1</sub>=R<sub>2</sub>=R<sub>4</sub>=H**3g** R<sub>3</sub>=Cl, R<sub>1</sub>=R<sub>2</sub>=R<sub>4</sub>=H**3h** R<sub>3</sub>=Br, R<sub>1</sub>=R<sub>2</sub>=R<sub>4</sub>=H**3i** R<sub>1</sub>=R<sub>3</sub>=F, R<sub>2</sub>=R<sub>4</sub>=H**3j** R<sub>1</sub>=R<sub>4</sub>=F, R<sub>2</sub>=R<sub>3</sub>=H**3k** R<sub>1</sub>=R<sub>2</sub>=R<sub>3</sub>=R<sub>4</sub>=H**3l** R<sub>1</sub>=NO<sub>2</sub>, R<sub>2</sub>=R<sub>3</sub>=R<sub>4</sub>=H**3m** R<sub>2</sub>=NO<sub>2</sub>, R<sub>1</sub>=R<sub>3</sub>=R<sub>4</sub>=H**3n** R<sub>3</sub>=NO<sub>2</sub>, R<sub>1</sub>=R<sub>2</sub>=R<sub>4</sub>=H**6a** R<sub>5</sub>=R<sub>6</sub>=R<sub>7</sub>=R<sub>8</sub>=H**6b** R<sub>7</sub>=OCH<sub>3</sub>, R<sub>5</sub>=R<sub>6</sub>=R<sub>8</sub>=H**6c** R<sub>7</sub>=NO<sub>2</sub>, R<sub>5</sub>=R<sub>6</sub>=R<sub>8</sub>=H**6d** R<sub>7</sub>=OH, R<sub>5</sub>=R<sub>6</sub>=R<sub>8</sub>=H**6e** R<sub>7</sub>=Br, R<sub>5</sub>=R<sub>6</sub>=R<sub>8</sub>=H**6f** R<sub>7</sub>=Cl, R<sub>5</sub>=R<sub>6</sub>=R<sub>8</sub>=H**6g** R<sub>7</sub>=F, R<sub>5</sub>=R<sub>6</sub>=R<sub>8</sub>=H**6h** R<sub>5</sub>=F, R<sub>6</sub>=R<sub>7</sub>=R<sub>8</sub>=H**6i** R<sub>6</sub>=F, R<sub>5</sub>=R<sub>7</sub>=R<sub>8</sub>=H**6j** R<sub>5</sub>=OH, R<sub>6</sub>=R<sub>7</sub>=H, R<sub>8</sub>=Br**6k** R<sub>5</sub>=OH, R<sub>6</sub>=R<sub>7</sub>=R<sub>8</sub>=H**6l** R<sub>5</sub>=OH, R<sub>6</sub>=R<sub>8</sub>=Br, R<sub>7</sub>=H**6m** R<sub>5</sub>=R<sub>8</sub>=H, R<sub>6</sub>=R<sub>7</sub>=OH**6n** A=C<sub>6</sub>H<sub>5</sub>-C=C-

bromine > chlorine > fluorine > nitro. Compounds with hydroxy at *ortho*-position had better inhibitory activity (**6j**, **6k**, **6l**). Overall, series **6a–6n** had better activities than series **3a–3n**. That might be caused by the additional hydrazone structure, and it will also be mentioned in the SARs study part.

In addition, we also selected the top 7 compounds which had better anti-proliferative activity to test their FAK inhibitory activity against HepG2 cell line. The results were summarized in Table 3. Most of the tested compounds displayed potent FAK inhibitory. Among them, compound **6j** showed the most potent inhibitory with IC<sub>50</sub> of 2.41 μM. The results of FAK inhibitory activity of the tested compounds were corresponding to the structure relationships of their anti-tumor activities. This demonstrated that the potent anti-tumor activities of the synthetic

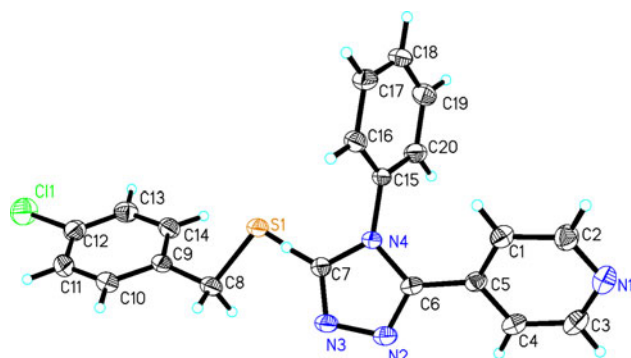
compounds were probably correlated to their FAK inhibitory activities.

#### Apoptosis assay

Apoptosis is an essential mechanism used to eliminate activated HCT116 cells during the shutdown process of excess immune responses and maintain proper immune homeostasis, while deficient apoptosis of the activated HCT116 cell is associated with a wide variety of immune disorders. We detected the mechanism of compounds **3e** and **6j** (Fig. 2) inhibition effects by flow cytometry, and found that the compounds could induce the apoptosis of activated HCT116 cells in a dose-dependent manner. The result indicated that compounds **3e** and **6j** induced apoptosis of anti-tumor stimulated HCT116 cells.

**Table 1** Crystallographical and experimental data for compound **3g**

Crystal parameters	Compound <b>3g</b>
Formula	C <sub>20</sub> H <sub>15</sub> ClN <sub>4</sub> S
Formula weight	378.07
Crystal size (mm)	0.2 × 0.1 × 0.1
α (°)	108.585(3)
β (°)	94.382(4)
γ (°)	91.66(4)
a (Å)	5.765(2)
b (Å)	12.280(5)
c (Å)	13.427(5)
V (Å <sup>3</sup> )	896.8(6)
Z	4
Calculated density (Mg cm <sup>-3</sup> )	1.751
Absorption coefficient (mm <sup>-1</sup> )	1.385
F (0 0 0)	470
θ range (°)	2.73–26.00
hkl limits	−7 ≤ h ≤ 7, −15 ≤ k ≤ 15, −16 ≤ l ≤ 16
Reflections collected/unique	6,642/3,452 [R <sub>int</sub> = 0.0256]
Data/restraints/parameters	3,452/0/235
R <sub>1</sub> /wR <sub>2</sub> [I > 2σ(I)]	0.0565/0.1762
R <sub>1</sub> /wR <sub>2</sub> (all data)	0.0829/0.1982
GOF	0.834

**Fig. 1** Molecule structure of compound **3g**

### Western-blot assay

In an effort to study the preliminary mechanism of the compounds with potent inhibitory activity, the western-blot experiment was performed to explore the effect of compounds **3e** and **6j**. The western-blot results were summarized in Fig. 3a and b, confirming compounds **3e** and **6j**'s inhibitory activities. The result indicated that compound **6j** showed excellent inhibitory activity.

**Table 2** Anti-proliferative activity of the synthesized compounds (**3a–3n** and **6a–6n**)

Compounds	IC <sub>50</sub> (μM)		
	MCF7	HCT116	HepG2
<b>3a</b>	>50	11.97	>50
<b>3b</b>	18.07	13.85	15.70
<b>3c</b>	16.06	20.15	17.11
<b>3d</b>	10.54	9.82	11.17
<b>3e</b>	10.04	8.17	7.04
<b>3f</b>	21.05	12.80	15.62
<b>3g</b>	13.27	10.70	16.94
<b>3h</b>	12.55	11.09	12.88
<b>3i</b>	14.10	11.39	10.15
<b>3j</b>	>50	22.10	>50
<b>3k</b>	22.38	16.91	12.91
<b>3l</b>	>50	>50	>50
<b>3m</b>	18.29	19.81	21.96
<b>3n</b>	22.84	23.82	>50
<b>6a</b>	23.64	14.68	18.60
<b>6b</b>	23.73	19.23	27.07
<b>6c</b>	15.28	10.18	15.89
<b>6d</b>	>50	>50	>50
<b>6e</b>	7.04	4.50	5.99
<b>6f</b>	9.93	5.74	10.95
<b>6g</b>	12.28	7.04	9.33
<b>6h</b>	22.43	18.04	15.17
<b>6i</b>	>50	>50	24.36
<b>6j</b>	6.46	1.99	4.39
<b>6k</b>	10.04	7.06	11.26
<b>6l</b>	8.44	4.50	7.59
<b>6m</b>	19.73	14.68	16.89
<b>6n</b>	11.17	6.15	8.28
Staurosporine	16.06	13.20	9.04

### Molecular docking study

To gain better understanding on the potency of the synthesized compounds and guide further SARs studies. The FAK-7PY protein–ligand complex crystal structure (PDB ID: 2ETM) was chosen as the template to compare the docking mode between our compounds and FAK. The molecular docking was performed by embedding potent inhibitors **3e** and **6j** into binding site of FAK. All docking runs were applied using Discovery Studio3.1 (DS. 3.1). In the binding mode, compound **3e** (Fig. 4) is bound to FAK via two π-cation interactions. One π-cation interaction (4.76 Å) is formed between LYS 454 and benzene ring while the other (6.19 Å) is formed between LYS 454 and triazole ring. In addition, compound **6j** (Fig. 4) is bound to

**Table 3** FAK inhibitory activity of selected compounds

Compound	FAK (IC <sub>50</sub> , μM)
<b>3e</b>	14.64
<b>3i</b>	17.38
<b>6e</b>	9.17
<b>6f</b>	11.98
<b>6g</b>	17.40
<b>6j</b>	2.41
<b>6n</b>	19.38
Staurosporine	3.12

FAK via one hydrogen bond and two π-cation interactions. Imino group on the acylhydrazone group and oxygen atom of CYS 502 form the hydrogen bond (distance: N–H···O: 2.35 Å, angle: 119.98°). Analogously, one π-cation interaction (4.79 Å) is formed between LYS 454 and benzene ring while the other (6.61 Å) is formed between LYS 454 and triazole ring. These results, along with the data of inhibitory activity assay indicated that compounds **3e** and **6j** would be a kind of potential inhibitors.

As the combinations shown in Fig. 5, Compound **2p** (Juan *et al.*, 2011) is nicely bound to FAK with two interactions. The amino hydrogen atom of LYS 454 forms

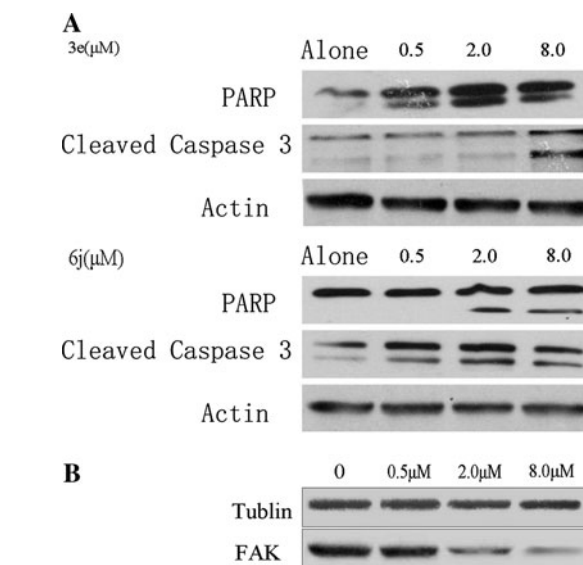


**Fig. 3** **a** Compounds **3e** and **6j** were examined by western blotting. Data are representative of three independent experiments. **b** Compounds **6j** were examined by western blotting. Data are representative of three independent experiments

a hydrogen bond with the oxygen atoms of 1,4-dioxane group. The nitrogen atom of amide group forms another hydrogen bond with the oxygen atom of CYS 502.

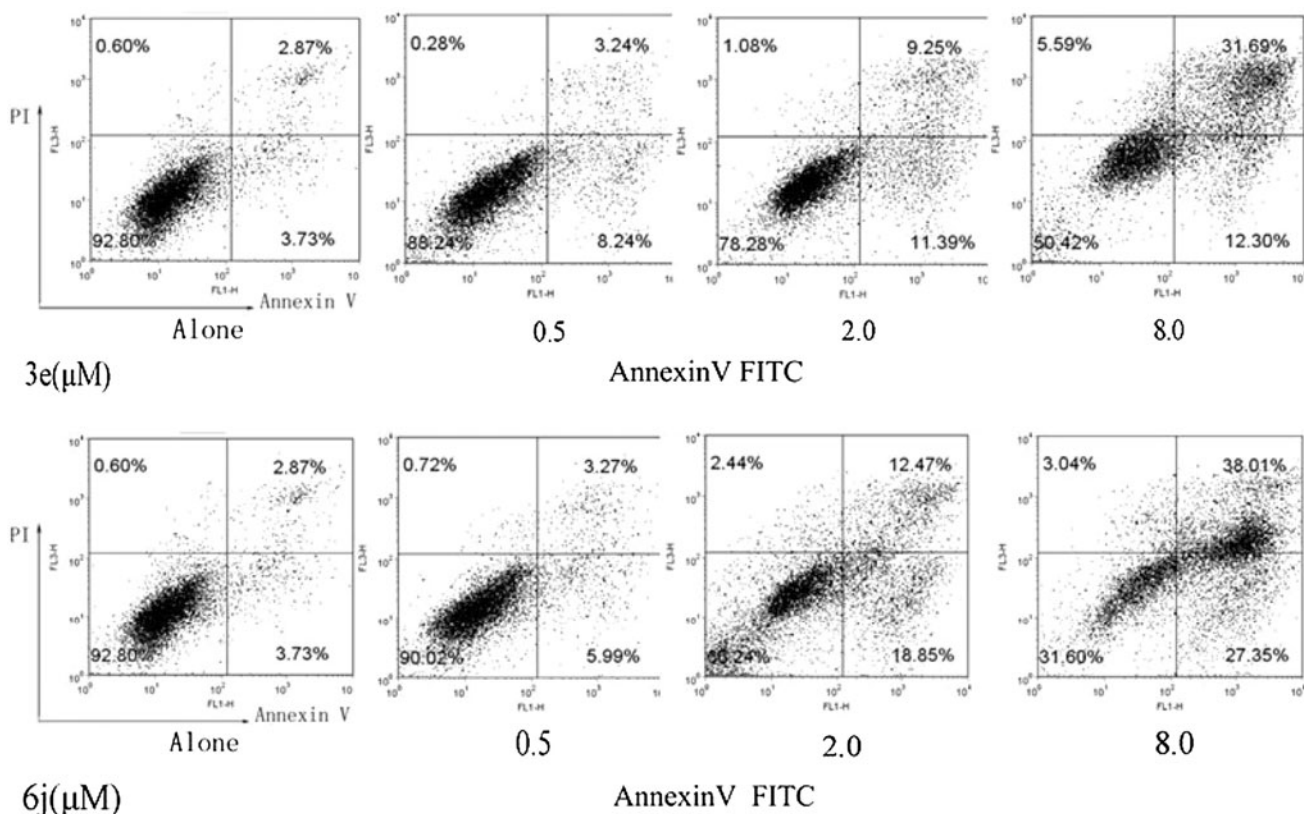


**Fig. 2** HCT116 cells isolated from naïve mice were cultured with anti-cancer and various concentrations of **3e** and **6j** for 24 h. Cells were stained by Annexin V/FITC/PI and apoptosis was analyzed by flow cytometry

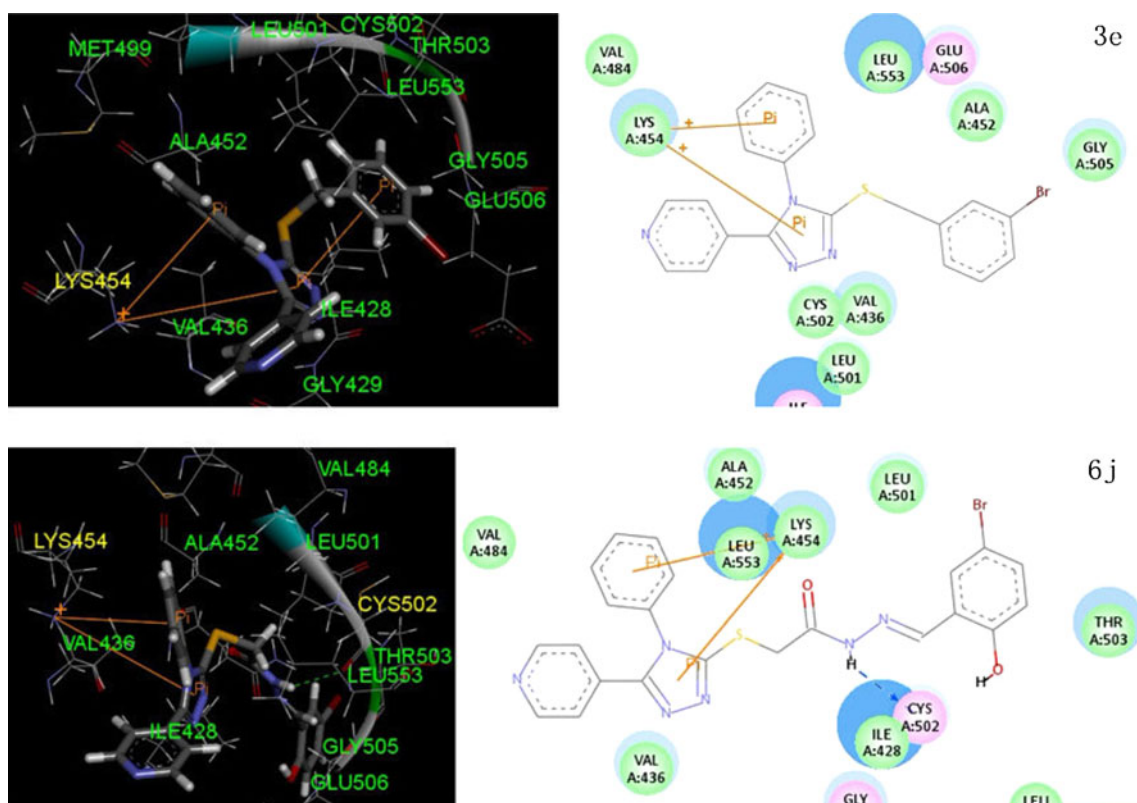


**Fig. 4** Molecular docking modeling of compounds **3e** and **6j** with FAK: for clarity, only interacting residues are displayed. *Left* 3D model of the interaction between compounds **3e**, **6j**, and the 2ETM binding site. The H-bond (green lines) is displayed as dotted lines, and the

$\pi$ -cation interactions are shown as orange lines. *Right* 2D model of the interaction between compound **3e**, **6j**, and the 2ETM binding site. The H-bond (blue arrows) is displayed as dotted arrows, and the  $\pi$ -cation interactions are shown as orange lines (Color figure online)

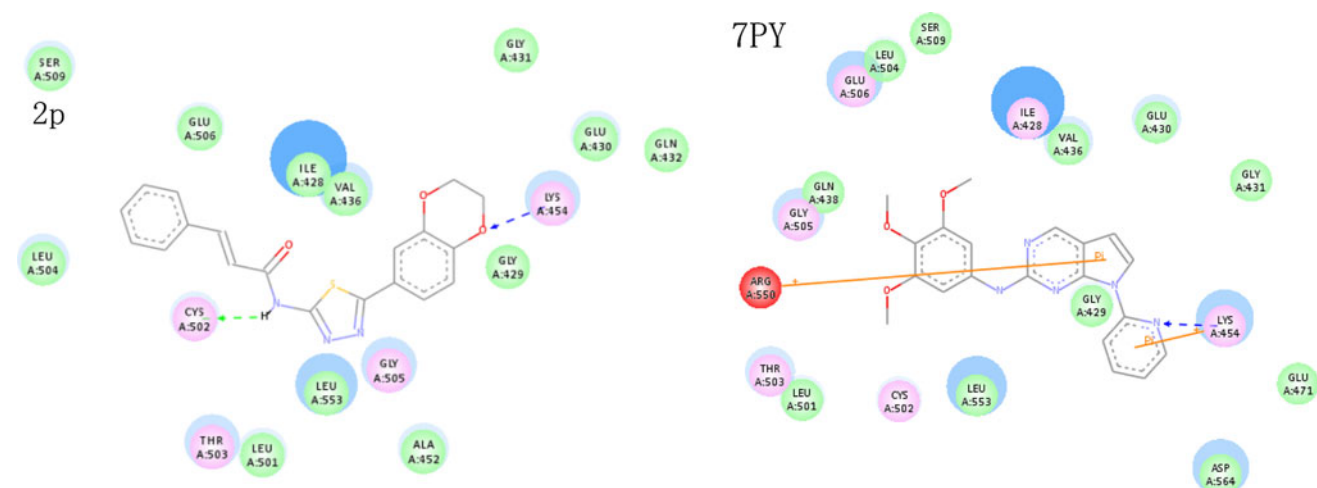


**Fig. 5** 2D model of the interaction between compounds **2p**, **7PY** and the 2ETM binding site. The H-bond is displayed as dotted arrows, and the  $\pi$ -cation interactions are shown as orange lines (Color figure online)

Compound **7PY** is also nicely bound to FAK with three interactions. The amino hydrogen atom of LYS 454 forms a hydrogen bond with the nitrogen atom of pyridine group. Also the pyridine ring of compound **7PY** forms a  $\pi$ -cation

interaction with LYS 454. Besides, the pyrrole ring of compound **7PY** forms a  $\pi$ -cation interaction with ARG 550. This insures the binding affinity and results in an increased FAK inhibitory activity.

In summary, the chosen 1,2,4-triazole derivatives containing pyridine are nicely combined to the FAK. LYS 454 and CYS 502 play an important part in the combination of the receptor and ligand.

## Conclusions

Two series of 1,2,4-triazole derivatives containing pyridine have been synthesized and evaluated for their anti-tumor activities. Compound **3e** and **6j** demonstrated the most potent inhibitory activity. **3e** inhibited the growth of the three cell lines with  $IC_{50}$  values range from 7.04 to 10.04  $\mu$ M, while **6j** inhibited the growth of the three cell lines with  $IC_{50}$  values range from 1.99 to 6.46  $\mu$ M. Besides **6j** also inhibited the activity of FAK with  $IC_{50}$  of 2.41  $\mu$ M, which was comparable to the positive control staurosporine. In order to gain deeper understanding of the SARs observed at the FAK, molecular docking of the most potent inhibitor **3e** and **6j** into the binding site of FAK was performed on the binding model based on the FAK complex structure. Analysis of the compound **6j**'s binding conformation demonstrated that compound **6j** was stabilized by hydrogen bonding interaction with CYS502. Apoptosis assay and western-blot results showed the compound **6j** was a potential anti-tumor agent.

## Experimental

### Cell proliferation assay

The anti-tumor activities of compounds **3a–3n** and **6a–6n** were determined using a standard (MTT)-based colorimetric assay (Sigma). Seed  $10^4$  cells per well into 96-well plates, incubate at 37 °C, 5 %  $CO_2$  for 24 h. Then add 100  $\mu$ L a series concentration of drug-containing medium into wells to maintain the final concentration of drug as 100, 30, 10, 3  $\mu$ M. One concentration should be triplicated. And staurosporine was used for the positive control. After 48 h, cell survival was determined by the addition of an MTT solution (25  $\mu$ L of 5 mg  $mL^{-1}$  MTT in PBS). After 4 h, discard the medium and add 100  $\mu$ L DMSO; the plates were vortexed for 10 min to make complete dissolution. Optical absorbance was measured at 490 nm.

### FAK inhibitory assay

Seven 1,2,4-triazole derivatives containing pyridine were tested in a search for small molecule inhibitors of FAK. In a typical study, human recombinant full-length FAK was incubated in kinase buffer containing ATP and the substrate for 4 h at room temperature with or without the presence of the triazole derivatives, the final concentration

of drug as 100, 30, 10, 3  $\mu$ M. The remaining ATP in solution was then quantified utilizing the Kinase-Glo-luminescence kit (Promega).

### Apoptosis assay

HCT116 cells were treated with various concentrations of compounds **3e** and **6j** for 24 h and then stained with both Annexin V-FITC (fluorescein isothiocyanate) and propidium iodide (PI). Then samples were analyzed by FACSCalibur flow cytometer (Becton–Dickinson, San Jose, CA).

### Western-blot analysis

After incubation, cells were washed with PBS and lysed using lysis buffer (30 mm Tris, pH 7.5, 150 mm NaCl, 1 mm phenylmethylsulfonyl fluoride, 1 mm  $Na_3VO_4$ , 1 % Nonidet P-40, 10 % glycerol, and phosphatase and protease inhibitors). After centrifugation at  $10,000 \times g$  for 10 min, the protein content of the supernatant was determined by a BCATM protein assay kit (Pierce, Rockford, IL, USA). The protein lysates were separated by 10 % SDS-PAGE and subsequently electrotransferred onto a polyvinylidene difluoride membrane (Millipore, Bedford, MA, USA). The membrane was blocked with 5 % non-fat milk for 2 h at room temperature. The blocked membrane was probed with the indicated primary antibodies overnight at 4 °C, and then incubated with a horse radish peroxidase-coupled secondary antibody. Detection was performed using a LumiGLO chemiluminescent substrate system (KPL, Guildford, UK).

### Molecular docking modeling

Molecular docking of compounds into the 3D FAK complex structure (PDB code: 2ETM) was carried out using the Discovery Studio (version 3.1) as implemented through the graphical user interface DS-CDocker protocol.

The three-dimensional structures of the aforementioned compounds were constructed using Chem 3D ultra 12.0 software [Chemical Structure Drawing Standard; Cambridge Soft corporation, USA (2010)], then they were energetically minimized using MMFF94 with 5000 iterations and minimum RMS gradient of 0.10. The crystal structures of FAK complex were retrieved from the RCSB Protein Data Bank (<http://www.rcsb.org/pdb/home/home.do>). All bound water and ligands were eliminated from the protein and the polar hydrogen was added. The whole FAK complex was defined as a receptor and the site sphere was selected based on the ligand binding location of **7PY**, then the **7PY** molecule was removed and **3e** and **6j** were placed during the molecular docking procedure. Types of interactions of the docked protein with ligand were analyzed after the end of molecular docking.

## Chemistry

All the NMR spectra were recorded on a Bruker DPX 300 model Spectrometer in CDCl<sub>3</sub>. Chemical shifts ( $\delta$ ) for <sup>1</sup>H NMR spectra were reported in parts per million to residual solvent protons. Melting points were measured on a Boettius micro melting point apparatus. The ESI–MS spectra were recorded on a Mariner System 5304 Mass spectrometer. All chemicals and reagents used in current study were of analytical grade. TLC was run on the silica gel coated aluminum sheets (Silica Gel 60 GF254, E. Merk, Germany) and visualized in UV light (254 nm).

General procedure for synthesis of the target compounds (**3a–3n**) and (**6a–6n**)

To a solution of compound **2** (1 mmol) in acetonitrile, the corresponding benzyl bromide compounds (1 mmol) were added and the mixture was stirred under reflux for 4–8 h in the presence of NaOH (2 mmol). Then, the solvent was removed under reduced pressure and a solid obtained. The solid was recrystallized from acetonitrile to afford compounds **3a–3n**.

To a stirred solution of compound **5** (1 mmol) and the corresponding benzaldehyde compounds (1 mmol) in ethanol (15 mL), water (1 mL) was added followed by dropwise addition of glacial acetic acid (0.2 mL). The resulting mixture was stirred at room temperature until the target product precipitate from the solvent, which was collected using suction filtration and dried. The solid was recrystallized from acetonitrile to afford compounds **6a–6n**.

*4-(5-((2-Fluorobenzyl)thio)-4-phenyl-4H-1,2,4-triazol-3-yl)pyridine (3a)*

Yellow solid, yield 83 %, mp: 173–174 °C. <sup>1</sup>H NMR (300 MHz, CDCl<sub>3</sub>): 4.62 (s, 2H); 7.02–7.12 (m, 2H); 7.24 (d,  $J = 11.52$  Hz, 1H); 7.31 (d,  $J = 5.28$  Hz, 1H); 7.51 (t,  $J = 7.78$  Hz, 1H); 7.61–7.70 (m, 4H); 7.92 (d,  $J = 6.24$  Hz, 2H); 8.64 (d,  $J = 6.22$  Hz, 2H). ESI–MS 363.1 (C<sub>20</sub>H<sub>16</sub>FN<sub>4</sub>S [M+H]<sup>+</sup>). Anal. Calcd for C<sub>20</sub>H<sub>15</sub>FN<sub>4</sub>S: C, 66.28; H, 4.17; N, 15.46. Found: C, 66.09; H, 4.16; N, 15.50.

*4-[5-(2-Chloro-benzylsulfanyl)-4-phenyl-4H-[1,2,4]triazol-3-yl]-pyridine (3b)*

Yellow solid, yield 87 %, mp: 139–140 °C. <sup>1</sup>H NMR (300 MHz, CDCl<sub>3</sub>): 4.63 (s, 2H); 7.12 (d,  $J = 8.26$  Hz, 2H); 7.19–7.23 (m, 2H); 7.28 (t,  $J = 3.78$  Hz, 2H); 7.33–7.37 (m, 1H); 7.49 (t,  $J = 6.96$  Hz, 3H); 7.55–7.59 (m, 1H); 8.53 (d,  $J = 6.02$  Hz, 2H). ESI–MS 379.1 (C<sub>20</sub>H<sub>16</sub>ClN<sub>4</sub>S [M+H]<sup>+</sup>). Anal. Calcd for C<sub>20</sub>H<sub>15</sub>ClN<sub>4</sub>S: C, 63.40; H, 3.99; N, 14.79. Found: C, 63.61; H, 4.00; N, 14.75.

*4-[5-(2-Bromo-benzylsulfanyl)-4-phenyl-4H-[1,2,4]triazol-3-yl]-pyridine (3c)*

Yellow solid, yield 79 %, mp: 145–146 °C. <sup>1</sup>H NMR (300 MHz, CDCl<sub>3</sub>): 4.64 (s, 2H); 7.20–7.31 (m, 2H); 7.61–7.70 (m, 5H); 7.80 (s, 2H); 8.18 (d,  $J = 8.76$  Hz, 2H); 8.60 (s, 2H). ESI–MS 423.0 (C<sub>20</sub>H<sub>16</sub>BrN<sub>4</sub>S [M+H]<sup>+</sup>). Anal. Calcd for C<sub>20</sub>H<sub>15</sub>BrN<sub>4</sub>S: C, 56.74; H, 3.57; N, 13.23. Found: C, 56.54; H, 3.56; N, 13.20.

*4-[5-(3-Chloro-benzylsulfanyl)-4-phenyl-4H-[1,2,4]triazol-3-yl]-pyridine (3d)*

Yellow solid, yield 81 %, mp: 149–150 °C. <sup>1</sup>H NMR (300 MHz, CDCl<sub>3</sub>): 4.47 (s, 2H); 7.13 (d,  $J = 6.30$  Hz, 2H); 7.18–7.28 (m, 3H); 7.33 (d,  $J = 6.76$  Hz, 3H); 7.49–7.60 (m, 3H); 8.54 (d,  $J = 6.06$  Hz, 2H). ESI–MS 379.1 (C<sub>20</sub>H<sub>16</sub>ClN<sub>4</sub>S [M+H]<sup>+</sup>). Anal. Calcd for C<sub>20</sub>H<sub>15</sub>ClN<sub>4</sub>S: C, 63.40; H, 3.99; N, 14.79. Found: C, 63.21; H, 4.00; N, 14.84.

*4-[5-(3-Bromo-benzylsulfanyl)-4-phenyl-4H-[1,2,4]triazol-3-yl]-pyridine (3e)*

White solid, yield 85 %, mp: 155–156 °C. <sup>1</sup>H NMR (300 MHz, CDCl<sub>3</sub>): 4.51 (s, 2H); 7.14–7.26 (m, 3H); 7.37 (dd,  $J_1 = 7.68$  Hz,  $J_2 = 11.70$  Hz, 2H); 7.54 (s, 1H); 7.59–7.68 (m, 3H); 7.86 (d,  $J = 6.76$  Hz, 2H); 8.75 (d,  $J = 6.76$  Hz, 2H). ESI–MS 423.0 (C<sub>20</sub>H<sub>16</sub>BrN<sub>4</sub>S [M+H]<sup>+</sup>). Anal. Calcd for C<sub>20</sub>H<sub>15</sub>BrN<sub>4</sub>S: C, 56.74; H, 3.57; N, 13.23. Found: C, 56.56; H, 3.58; N, 13.27.

*4-(5-((4-Fluorobenzyl)thio)-4-phenyl-4H-1,2,4-triazol-3-yl)pyridine (3f)*

Yellow solid, yield 77 %, mp: 142–143 °C. <sup>1</sup>H NMR (300 MHz, CDCl<sub>3</sub>): 4.53 (s, 2H); 6.91–7.00 (m, 2H); 7.14 (m, 2H); 7.35–7.40 (m, 4H); 7.50–7.61 (m, 3H); 8.55 (d,  $J = 6$  Hz, 2H). ESI–MS 363.1 (C<sub>20</sub>H<sub>16</sub>FN<sub>4</sub>S [M+H]<sup>+</sup>). Anal. Calcd for C<sub>20</sub>H<sub>15</sub>FN<sub>4</sub>S: C, 66.28; H, 4.17; N, 15.46. Found: C, 66.06; H, 4.18; N, 15.51.

*4-[5-(4-Chloro-benzylsulfanyl)-4-phenyl-4H-[1,2,4]triazol-3-yl]-pyridine (3g)*

White solid, yield 84 %, mp: 143–144 °C. <sup>1</sup>H NMR (300 MHz, CDCl<sub>3</sub>): 4.47 (s, 2H); 7.14 (d,  $J = 7.22$  Hz, 2H); 7.26 (d,  $J = 9.34$  Hz, 2H); 7.31 (t,  $J = 7.01$  Hz, 4H); 7.49–7.56 (m, 3H); 8.54 (d,  $J = 6.04$  Hz, 2H). ESI–MS 379.1 (C<sub>20</sub>H<sub>16</sub>ClN<sub>4</sub>S [M+H]<sup>+</sup>). Anal. Calcd for C<sub>20</sub>H<sub>15</sub>ClN<sub>4</sub>S: C, 63.40; H, 3.99; N, 14.79. Found: C, 63.24; H, 3.98; N, 14.74.

*4-[5-(4-Bromo-benzylsulfanyl)-4-phenyl-4H-[1,2,4]triazol-3-yl]-pyridine (3h)*

Yellow solid, yield 78 %, mp: 144–145 °C. <sup>1</sup>H NMR (300 MHz, CDCl<sub>3</sub>): 4.46 (s, 2H); 7.14 (d, *J* = 8.14 Hz, 2H); 7.24 (s, 1H); 7.27 (s, 1H); 7.37 (s, 1H); 7.40 (d, *J* = 9.50 Hz, 3H); 7.49–7.60 (m, 3H); 8.55 (s, 2H). ESI-MS 423.0 (C<sub>20</sub>H<sub>15</sub>BrN<sub>4</sub>S [M+H]<sup>+</sup>). Anal. Calcd for C<sub>20</sub>H<sub>15</sub>BrN<sub>4</sub>S: C, 56.74; H, 3.57; N, 13.23. Found: C, 56.55; H, 3.58; N, 13.28.

*4-(5-((2,4-Difluorobenzyl)thio)-4-phenyl-4H-1,2,4-triazol-3-yl)pyridine (3i)*

Yellow solid, yield 80 %, mp: 172–173 °C. <sup>1</sup>H NMR (300 MHz, CDCl<sub>3</sub>): 4.55 (s, 2H); 6.80–6.83 (m, 2H); 7.20–7.23 (m, 2H); 7.58–7.64 (m, 6H); 8.57 (d, *J* = 6.42 Hz, 2H). ESI-MS 381.1 (C<sub>20</sub>H<sub>15</sub>F<sub>2</sub>N<sub>4</sub>S [M+H]<sup>+</sup>). Anal. Calcd for C<sub>20</sub>H<sub>14</sub>F<sub>2</sub>N<sub>4</sub>S: C, 63.15; H, 3.71; N, 14.73. Found: C, 63.33; H, 3.72; N, 14.78.

*4-[5-(2,6-Difluoro-benzylsulfanyl)-4-phenyl-4H-[1,2,4]triazol-3-yl]-pyridine (3j)*

Yellow solid, yield 82 %, mp: 142–143 °C. <sup>1</sup>H NMR (300 MHz, CDCl<sub>3</sub>): 4.62 (s, 2H); 7.01–7.11 (m, 2H); 7.21–7.29 (m, 2H); 7.51 (t, *J* = 7.68 Hz, 2H); 7.59–7.68 (m, 2H); 7.87 (s, 2H); 8.62 (d, *J* = 6.76 Hz, 2H). ESI-MS 381.1 (C<sub>20</sub>H<sub>15</sub>F<sub>2</sub>N<sub>4</sub>S [M+H]<sup>+</sup>). Anal. Calcd for C<sub>20</sub>H<sub>14</sub>F<sub>2</sub>N<sub>4</sub>S: C, 63.15; H, 3.71; N, 14.73. Found: C, 63.37; H, 3.70; N, 14.78.

*4-(5-(Benzylthio)-4-phenyl-4H-1,2,4-triazol-3-yl)pyridine (3k)*

White solid, yield 86 %, mp: 155–156 °C. <sup>1</sup>H NMR (300 MHz, CDCl<sub>3</sub>): 4.53 (s, 2H); 7.12–7.14 (m, 2H); 7.27–7.30 (m, 3H); 7.40–7.42 (m, 4H); 7.49–7.57 (m, 3H); 8.54 (d, *J* = 6.18 Hz, 2H). ESI-MS 345.1 (C<sub>20</sub>H<sub>17</sub>N<sub>4</sub>S [M+H]<sup>+</sup>). Anal. Calcd for C<sub>20</sub>H<sub>16</sub>N<sub>4</sub>S: C, 69.74; H, 4.68; N, 16.27. Found: C, 69.50; H, 4.69; N, 16.33.

*4-[5-(2-Nitro-benzylsulfanyl)-4-phenyl-4H-[1,2,4]triazol-3-yl]-pyridine (3l)*

Yellow solid, yield 82 %, mp: 141 °C. <sup>1</sup>H NMR (300 MHz, CDCl<sub>3</sub>): 4.89 (s, 2H); 7.14 (d, *J* = 6.78 Hz, 2H); 7.33 (d, *J* = 4.66 Hz, 2H); 7.43–7.62 (m, 5H); 7.94 (d, *J* = 7.68 Hz, 1H); 8.08 (d, *J* = 8.22 Hz, 1H); 8.53 (d, *J* = 6.24 Hz, 2H). ESI-MS 390.1 (C<sub>20</sub>H<sub>15</sub>N<sub>2</sub>O<sub>2</sub>S [M+H]<sup>+</sup>). Anal. Calcd for C<sub>20</sub>H<sub>15</sub>N<sub>2</sub>O<sub>2</sub>S: C, 61.68; H, 3.88; N, 17.98. Found: C, 61.48, H, 3.89; N, 18.04.

*4-[5-(3-Nitro-benzylsulfanyl)-4-phenyl-4H-[1,2,4]triazol-3-yl]-pyridine (3m)*

Yellow solid, yield 80 %, mp: 154–155 °C. <sup>1</sup>H NMR (300 MHz, CDCl<sub>3</sub>): 4.59 (s, 2H); 7.17 (d, *J* = 7.50 Hz, 2H); 7.28 (t, *J* = 5.86 Hz, 2H); 7.46–7.58 (m, 4H); 7.81 (d, *J* = 7.68, 1H); 8.12 (d, *J* = 7.32 Hz, 1H); 8.25 (s, 1H); 8.53 (d, *J* = 5.68 Hz, 2H). ESI-MS 390.1 (C<sub>20</sub>H<sub>15</sub>N<sub>5</sub>O<sub>2</sub>S [M+H]<sup>+</sup>). Anal. Calcd for C<sub>20</sub>H<sub>15</sub>N<sub>5</sub>O<sub>2</sub>S: C, 61.68; H, 3.88; N, 17.98. Found: C, 61.82; H, 3.89; N, 18.04.

*4-[5-(4-Nitro-benzylsulfanyl)-4-phenyl-4H-[1,2,4]triazol-3-yl]-pyridine (3n)*

Yellow solid, yield 77 %, mp: 90–91 °C. <sup>1</sup>H NMR (300 MHz, CDCl<sub>3</sub>): 4.59 (s, 2H); 7.18 (d, *J* = 6.96 Hz, 2H); 7.38 (d, *J* = 5.86 Hz, 2H); 7.53–7.63 (m, 5H); 8.16 (d, *J* = 8.80 Hz, 2H); 8.55 (d, *J* = 6.04 Hz, 2H). ESI-MS 390.1 (C<sub>20</sub>H<sub>16</sub>N<sub>5</sub>O<sub>2</sub>S [M+H]<sup>+</sup>). Anal. Calcd for C<sub>20</sub>H<sub>15</sub>N<sub>5</sub>O<sub>2</sub>S: C, 61.68; H, 3.88; N, 17.98. Found: C, 61.51; H, 3.89; N, 18.03.

*(E)-N'-benzylidene-2-((4-phenyl-5-(pyridin-4-yl)-4H-1,2,4-triazol-3-yl)thio)acetohydrazide (6a)*

White powder, yield 87 %; mp: 252–253 °C. <sup>1</sup>H NMR (300 MHz, DMSO): 4.52 (s, 2H); 7.30 (s, 2H); 7.45 (s, 1H); 7.50–7.52 (m, 4H); 7.61–7.62 (m, 3H); 7.69–7.73 (m, 2H); 8.01 (s, 1H); 8.57 (s, 2H); 11.73 (s, 1H). ESI-MS: 415.1 (C<sub>22</sub>H<sub>19</sub>N<sub>6</sub>OS, [M+H]<sup>+</sup>). Anal. Calcd for C<sub>22</sub>H<sub>18</sub>N<sub>6</sub>OS: C, 63.75; H, 4.38; N, 20.28 %. Found: C, 63.58; H, 4.39; N, 20.22 %.

*(E)-N'-(4-methoxybenzylidene)-2-((4-phenyl-5-(pyridin-4-yl)-4H-1,2,4-triazol-3-yl)thio)acetohydrazide (6b)*

White powder, yield 90 %; mp: 228–229 °C. <sup>1</sup>H NMR (300 MHz, DMSO): 3.79 (s, 3H); 4.50 (s, 2H); 6.97–6.99 (m, 2H); 7.26–7.28 (m, 2H); 7.48 (s, 2H); 7.59–7.64 (m, 5H); 7.94 (s, 1H); 8.54–8.55 (m, 2H); 11.56 (s, 1H). ESI-MS: 445.1 (C<sub>23</sub>H<sub>21</sub>N<sub>6</sub>O<sub>2</sub>S, [M+H]<sup>+</sup>). Anal. Calcd for C<sub>23</sub>H<sub>20</sub>N<sub>6</sub>O<sub>2</sub>S: C, 62.15; H, 4.54; N, 18.91. Found: C, 62.35; H, 4.53; N, 18.85.

*(E)-N'-(4-nitrobenzylidene)-2-((4-phenyl-5-(pyridin-4-yl)-4H-1,2,4-triazol-3-yl)thio)acetohydrazide (6c)*

White powder, yield 91 %; mp: 248–249 °C. <sup>1</sup>H NMR (300 MHz, DMSO): 4.56 (s, 2H); 7.26 (s, 2H); 7.48 (s, 2H); 7.59–7.60 (m, 3H); 7.92–7.97 (m, 2H); 8.11–8.31 (m, 3H); 8.54 (s, 2H); 11.95 (s, 1H). ESI-MS: 460.1 (C<sub>22</sub>H<sub>18</sub>N<sub>7</sub>O<sub>3</sub>S, [M+H]<sup>+</sup>). Anal. Calcd for C<sub>22</sub>H<sub>17</sub>N<sub>7</sub>O<sub>3</sub>S:

C, 57.51; H, 3.73; N, 21.34. Found: C, 57.35; H, 3.72; N, 21.41.

(*E*)-*N'*-(4-hydroxybenzylidene)-2-((4-phenyl-5-(pyridin-4-yl)-4*H*-1,2,4-triazol-3-yl)thio)acetohydrazide (**6d**)

White powder, yield 93 %; mp: 284–285 °C. <sup>1</sup>H NMR (300 MHz, DMSO): 4.48 (s, 2H); 6.79 (d, *J* = 4.95 Hz, 2H); 7.25–7.26 (m, 2H); 7.47–7.51 (m, 4H); 7.59 (s, 3H); 7.89 (s, 1H); 8.53 (s, 2H); 9.88 (s, 1H); 11.45 (s, 1H). ESI-MS: 431.1 (C<sub>22</sub>H<sub>19</sub>N<sub>6</sub>O<sub>2</sub>S, [M+H]<sup>+</sup>). Anal. Calcd for C<sub>22</sub>H<sub>18</sub>N<sub>6</sub>O<sub>2</sub>S: C, 61.38; H, 4.21; N, 19.52. Found: C, 61.58; H, 4.22; N, 19.45.

(*E*)-*N'*-(4-bromobenzylidene)-2-((4-phenyl-5-(pyridin-4-yl)-4*H*-1,2,4-triazol-3-yl)thio)acetohydrazide (**6e**)

White powder, yield 89 %; mp: 232–233 °C. <sup>1</sup>H NMR (300 MHz, DMSO): 4.53 (s, 2H); 7.27–7.29 (m, 2H); 7.50 (s, 2H); 7.62–7.65 (m, 7H); 8.00 (s, 1H); 8.55 (d, *J* = 3 Hz, 2H); 11.75 (s, 1H). ESI-MS: 493.0 (C<sub>22</sub>H<sub>18</sub>BrN<sub>6</sub>OS, [M+H]<sup>+</sup>). Anal. Calcd for C<sub>22</sub>H<sub>17</sub>BrN<sub>6</sub>OS: C, 53.56; H, 3.47; N, 17.03. Found: C, 53.41; H, 3.46; N, 17.07.

(*E*)-*N'*-(4-chlorobenzylidene)-2-((4-phenyl-5-(pyridin-4-yl)-4*H*-1,2,4-triazol-3-yl)thio)acetohydrazide (**6f**)

White powder, yield 92 %; mp: 218–219 °C. <sup>1</sup>H NMR (300 MHz, DMSO): 4.53 (s, 2H); 7.28 (*t*, *J* = 5.1 Hz, 2H); 7.50–7.51 (m, 4H); 7.62 (s, 3H); 7.69–7.73 (m, 2H); 8.01 (s, 1H); 8.55 (s, 2H); 11.73 (s, 1H). ESI-MS: 449.1 (C<sub>22</sub>H<sub>18</sub>ClN<sub>6</sub>OS, [M+H]<sup>+</sup>). Anal. Calcd for C<sub>22</sub>H<sub>17</sub>ClN<sub>6</sub>OS: C, 58.86; H, 3.82; N, 18.72. Found: C, 58.69; H, 3.83; N, 18.77.

(*E*)-*N'*-(4-fluorobenzylidene)-2-((4-phenyl-5-(pyridin-4-yl)-4*H*-1,2,4-triazol-3-yl)thio)acetohydrazide (**6g**)

White powder, yield 90 %; mp: 227–228 °C. <sup>1</sup>H NMR (300 MHz, DMSO): 4.54 (s, 2H); 7.30 (s, 2H); 7.50–7.51 (m, 4H); 7.61–7.62 (m, 3H); 7.69–7.73 (m, 2H); 8.01 (s, 1H); 8.57 (s, 2H); 11.75 (s, 1H). ESI-MS: 433.1 (C<sub>22</sub>H<sub>18</sub>FN<sub>6</sub>OS, [M+H]<sup>+</sup>). Anal. Calcd for C<sub>22</sub>H<sub>17</sub>FN<sub>6</sub>OS: C, 61.10; H, 3.96; N, 19.43. Found: C, 61.29; H, 3.95; N, 19.49.

(*E*)-*N'*-(2-fluorobenzylidene)-2-((4-phenyl-5-(pyridin-4-yl)-4*H*-1,2,4-triazol-3-yl)thio)acetohydrazide (**6h**)

White powder, yield 91 %; mp: 235–236 °C. <sup>1</sup>H NMR (300 MHz, DMSO): 4.41 (s, 2H); 6.95–7.11 (m, 2H); 7.29–7.32 (m, 3H); 7.37–7.39 (m, 2H); 7.51 (s, 2H); 7.60–7.62 (m, 2H); 7.82 (s, 1H); 8.54 (s, 2H); 11.59 (s, 1H). ESI-MS: 433.1 (C<sub>22</sub>H<sub>18</sub>FN<sub>6</sub>OS, [M+H]<sup>+</sup>). Anal.

Calcd for C<sub>22</sub>H<sub>17</sub>FN<sub>6</sub>OS: C, 61.10; H, 3.96; N, 19.43. Found: C, 61.27; H, 3.95; N, 19.37.

(*E*)-*N'*-(3-fluorobenzylidene)-2-((4-phenyl-5-(pyridin-4-yl)-4*H*-1,2,4-triazol-3-yl)thio)acetohydrazide (**6i**)

White powder, yield 89 %; mp: 227–228 °C. <sup>1</sup>H NMR (300 MHz, DMSO): 4.55 (s, 2H); 7.30 (s, 2H); 7.50–7.52 (m, 4H); 7.60–7.62 (m, 3H); 7.70–7.73 (m, 2H); 8.01 (s, 1H); 8.55 (s, 2H); 11.71 (s, 1H). ESI-MS: 433.1 (C<sub>22</sub>H<sub>18</sub>FN<sub>6</sub>OS, [M+H]<sup>+</sup>). Anal. Calcd for C<sub>22</sub>H<sub>17</sub>FN<sub>6</sub>OS: C, 61.10; H, 3.96; N, 19.43. Found: C, 61.28; H, 3.95; N, 19.47.

(*E*)-*N'*-(2-hydroxybenzylidene)-2-((4-phenyl-5-(pyridin-4-yl)-4*H*-1,2,4-triazol-3-yl)thio)acetohydrazide (**6j**)

White powder, yield 88 %; mp: 242–243 °C. <sup>1</sup>H NMR (300 MHz, DMSO): 4.52 (s, 2H); 6.85–6.92 (m, 2H); 7.23–7.30 (m, 3H); 7.50–7.66 (m, 6H); 8.42 (s, 1H); 8.50 (s, 2H); 10.95 (s, 1H); 11.99 (s, 1H). ESI-MS: 331.1 (C<sub>22</sub>H<sub>19</sub>N<sub>6</sub>O<sub>2</sub>S, [M+H]<sup>+</sup>). Anal. Calcd for C<sub>22</sub>H<sub>18</sub>N<sub>6</sub>O<sub>2</sub>S: C, 61.38; H, 4.21; N, 19.52. Found: C, 61.57; H, 4.20; N, 19.46.

(*E*)-*N'*-(5-bromo-2-hydroxybenzylidene)-2-((4-phenyl-5-(pyridin-4-yl)-4*H*-1,2,4-triazol-3-yl)thio)acetohydrazide (**6j**)

White powder, yield 90 %; mp: 290–291 °C. <sup>1</sup>H NMR (300 MHz, DMSO): 4.50 (s, 2H); 6.86–6.91 (m, 2H); 7.25–7.30 (m, 2H); 7.53–7.67 (m, 6H); 8.46 (s, 1H); 8.51 (s, 2H); 10.97 (s, 1H); 11.97 (s, 1H). ESI-MS: 509.0 (C<sub>22</sub>H<sub>18</sub>BrN<sub>6</sub>O<sub>2</sub>S, [M+H]<sup>+</sup>). Anal. Calcd for C<sub>22</sub>H<sub>17</sub>BrN<sub>6</sub>O<sub>2</sub>S: C, 51.87; H, 3.36; N, 16.50. Found: C, 51.68; H, 3.37; N, 16.55.

(*E*)-*N'*-(3,5-dibromo-2-hydroxybenzylidene)-2-((4-phenyl-5-(pyridin-4-yl)-4*H*-1,2,4-triazol-3-yl)thio)acetohydrazide (**6k**)

White powder, yield 88 %; mp: 270–271 °C. <sup>1</sup>H NMR (300 MHz, DMSO): 4.53 (s, 2H); 6.83–6.87 (m, 2H); 7.26–7.30 (m, 2H); 7.55–7.65 (m, 5H); 8.43 (s, 1H); 8.52 (s, 2H); 10.99 (s, 1H); 12.01 (s, 1H). ESI-MS: 586.9 (C<sub>22</sub>H<sub>17</sub>Br<sub>2</sub>N<sub>6</sub>O<sub>2</sub>S, [M+H]<sup>+</sup>). Anal. Calcd for C<sub>22</sub>H<sub>16</sub>Br<sub>2</sub>N<sub>6</sub>O<sub>2</sub>S: C, 44.92; H, 2.74; N, 14.29. Found: C, 44.78; H, 2.73; N, 14.34.

(*E*)-*N'*-(3,4-dihydroxybenzylidene)-2-((4-phenyl-5-(pyridin-4-yl)-4*H*-1,2,4-triazol-3-yl)thio)acetohydrazide (**6m**)

White powder, yield 92 %; mp: 255–256 °C. <sup>1</sup>H NMR (300 MHz, DMSO): 3.41–3.45 (m, 2H); 4.54 (s, 2H); 6.77

(d,  $J = 4.83$  Hz, 1H); 6.89 (t,  $J = 5.88$  Hz, 1H); 7.16 (d,  $J = 10.44$  Hz, 1H); 7.49–7.50 (m, 2H); 7.53–7.54 (m, 2H); 7.62–7.64 (m, 3H); 7.84 (s, 1H); 8.67–8.69 (m, 2H); 11.47 (s, 1H). ESI-MS: 447.1 ( $C_{22}H_{19}N_6O_3S$ ,  $[M+H]^+$ ). Anal. Calcd for  $C_{22}H_{18}N_6O_3S$ : C, 59.18; H, 4.06; N, 18.82. Found: C, 59.01; H, 4.05; N, 18.77.

(*E*)-2-((4-phenyl-5-(pyridin-4-yl)-4*H*-1,2,4-triazol-3-yl)thio)-*N'*-((*E*)-3-phenylallylidene)acetohydrazide (**6n**)

White powder, yield 92 %; mp: 235–236 °C.  $^1H$  NMR (300 MHz, DMSO): 4.45 (s, 2H); 6.93–7.10 (m, 2H); 7.29–7.33 (m, 3H); 7.36–7.39 (m, 2H); 7.51 (s, 2H); 7.61–7.62 (m, 5H); 7.83 (d,  $J = 5.88$  Hz, 1H); 8.54 (s, 2H); 11.59 (s, 1H). ESI-MS: 441.1 ( $C_{24}H_{21}N_6OS$ ,  $[M+H]^+$ ). Anal. Calcd for  $C_{24}H_{20}N_6OS$ : C, 65.44; H, 4.58; N, 19.08. Found: C, 65.59; H, 4.57; N, 19.14.

**Acknowledgments** The study was financed by National Natural Science Foundation of China (No. J1103512) and Dr. Qiu thanks Henan Research Program of Foundation and Advanced Technology (112300410324, 122300410386).

## References

- Almasirad A, Tabatabai SA, Faizi M, Kebriaeezadeh A, Mehrabi N, Dalvandi A, Shafiee A (2004) Synthesis and anticonvulsant activity of new 2-substituted-5-[2-(2-fluorophenoxy)phenyl]-1,3,4-oxadiazoles and 1,2,4-triazoles. *Bioorg Med Chem Lett* 14:6057–6059
- Amir M, Shikha K (2004) Synthesis and anti-inflammatory, analgesic, ulcerogenic and lipid peroxidation activities of some new 2-[(2,6-dichloroanilino) phenyl]acetic acid derivatives. *Eur J Med Chem* 39:535–545
- Aronsohn MS, Brown HM, Hauptman G, Kornberg LJ (2003) Expression of focal adhesion kinase and phosphorylated focal adhesion kinase in squamous cell carcinoma of the larynx. *Laryngoscope* 113:1944–1948
- Ashok M, Holla BS (2007) Convenient synthesis of some triazolothiadiazoles and triazolothiadiazines carrying 4-methylthiobenzyl moiety as possible antimicrobial agents. *J Pharmacol Toxicol* 2:256–263
- Bhat KS, Poojary B, Prasad DJ, Nalk B, Holla BS (2009) Synthesis and antitumor activity studies of some new fused 1,2,4-triazole derivatives carrying 2,4-dichloro-5-fluorophenyl moiety. *Eur J Med Chem* 44:5066–5070
- Budavari S, O'Neil MJ, Smith A, Heckelman PE, Kinneary JF (1996) The Merck index, an encyclopedia of chemicals, drugs, and biologicals, 12th edn. Merck & Co., Inc., Whitehouse Station, NJ
- El-Azab AS, Al-Omar MA, Abdel-Aziz AM, Abdel-Aziz NI, El-Sayed AA, Aleisa AM, Sayed-Ahmed MM, Abdel-Hamide SG (2010) Design, synthesis and biological evaluation of novel quinazoline derivatives as potential antitumor agents: molecular docking study. *Eur J Med Chem* 45:4188–4198
- Golubovskaya V, Kaur A, Cance W (2004) Cloning and characterization of the promoter region of human focal adhesion kinase gene: nuclear factor kappaB and p53 binding sites. *Biochim Biophys Acta* 1678:111–125
- Haber J (2001) Present status and perspectives on antimycotics with systemic effects. *Cas Lek Cesk* 140:596–604
- Hanahan D, Weinberg RA (2000) The hallmarks of cancer. *Cell* 100:57–70
- Juan S, Yu-Shun Y, Wei L, Yan-bin Z, Xiao-Liang W, Jian-Feng T, Hai-Liang Z (2011) Synthesis, biological evaluation and molecular docking studies of 1,3,4-thiadiazole derivatives containing 1,4-benzodioxan as potential antitumor agents. *Bioorg Med Chem* 21:6116–6121
- Kahana O, Micksche M, Witz IP, Yron I (2002) The focal adhesion kinase (P125<sup>FAK</sup>) is constitutively active in human malignant melanoma. *Oncogene* 21:3969–3977
- Owens LV, Xu L, Craven RJ, Dent GA, Weiner TM, Kornberg L, Liu ET, Cance WG (1995) Overexpression of the focal adhesion kinase (p125<sup>FAK</sup>) in invasive human tumors. *Cancer Res* 55:2752
- Prasad DJ, Ashok M, Karegoudar P, Poojary B, Holla BS, Sucheta Kumari N (2009) Synthesis and antimicrobial activities of some new triazolothiadiazoles bearing 4-methylthiobenzyl moiety. *Eur J Med Chem* 44:551–557
- Romagnoli R, Baraldi PG (2010) Synthesis and antitumor activity of 1,5-disubstituted 1,2,4-triazoles as *cis*-restricted combretastatin analogues. *J Med Chem* 53:4248–4258
- Schreier E, Helv (1976) Human plasma levels of some anti-migraine drugs. *Chim Acta* 59:585–606
- Sheldrick GM (1997) SHELX-97. Program for X-ray crystal structure solution and refinement
- Sonoda Y, Matsumoto Y, Funakoshi M, Yamamoto D, Hanks SK, Kasahara T (2000) Anti-apoptotic role of focal adhesion kinase (FAK). Induction of inhibitor-of-apoptosis proteins and apoptosis suppression by the overexpression of FAK in a human leukemic cell line, HL-60. *J Biol Chem* 275:16309–16315
- Stanton HLK, Robeto G, Chung HC, Marcus CWY, Eva L (2008) Synthesis and anti-cancer activity of benzothiazole containing phthalimide on human carcinoma cell lines. *Bioorg Med Chem* 16:3626–3631
- Sztanke K, Tuzimski T (2008) Synthesis, determination of the lipophilicity, anticancer and antimicrobial properties of some fused 1,2,4-triazole derivatives. *Eur J Med Chem* 43:404–419
- Van Nimwegen MJ, van de Water B (2007) Focal adhesion kinase: a potential target in cancer therapy. *Biochem Pharmacol* 73:597–609
- Walczak K, Gondela A, Suwinski J (2004) Synthesis and anti-tuberculosis activity of *N*-aryl-*C*-nitroazoles. *Eur J Med Chem* 39:849–853